Grassmannian Delay-Tolerant Limited Feedback for Interference Alignment

Zhinan Xu, Thomas Zemen
FTW (Telecommunications Research Center Vienna)
Vienna, Austria
Email: {xu, thomas.zemen}@ftw.at

***Abstract*—In this paper, we propose a delay-tolerant limited feedback algorithm for single-input single-output (SISO) interference alignment. The temporal correlation and band limitation of the time-selective fading process is exploited to model the channel impulse response with a low-dimensional basis expansion. The algorithm tracks and feeds back the evolution of the basis expansion coefficients on the Grassmannian manifold. These coefficients allow the transmitter to predict the future channel realizations to compensate the feedback delay. By feeding back the quantized basis expansion coefficients instead of the channel impulse responses, the number of feedback bits can be substantially reduced. Our numerical results demonstrate that by exploiting the subspace structure of the time-variant channel we can reduce the amount of feedback to 2 bits per channel realization.**

I. Introduction

Interference is a crucial limitation in next generation cellular systems. To address this problem, interference alignment (IA) has attracted much attention and has been extensively studied lately. IA is able to achieve the optimal degrees of freedom (DoF) at high signal-to-noise ratio (SNR) and a rate of $K/2 \cdot \log(\mathrm{SNR}) + o(\log(\mathrm{SNR}))$ for the K user interference channel with time-variant coefficients [1]. However, this result is based on the assumption that *global* channel state information (CSI) is perfectly known at all nodes, which is extremely hard to achieve due to the large amount of required feedback information. Limited CSI feedback [2] is a reasonable approach to obtain CSI at the transmitter side, which can be only observed at the receiver side in frequency division duplex (FDD) systems.

Several works investigate the CSI feedback and the impact of channel quantization error on IA. The authors of [3] design an iterative algorithm which exploits channel reciprocity in wireless networks to achieve IA with only local CSI at each node. However channel reciprocity can be only utilized for time division duplexing (TDD) systems. For FDD systems, IA can also be achieved by opportunistic user selection exploiting the random channel for each individual user [4]. It is shown that with this approach the feedback information can be reduced to a single scalar for each user, and the achieved DoF scales with the number of active user candidates. In [5], blind interference alignment shows the ability to achieve IA without any CSI at the transmitter by exploiting the coherence structures associated with different users. However, the work is designed for multiple-input multiple-output (MIMO) broadcast channels and requires a strong assumption on the channel coherence structure.

To reduce the number of feedback bits [6] and [7] quantize channel coefficients using a Grassmannian codebook for frequency-selective single-input single-output (SISO) as well as MIMO channels. It is shown that the full DoF are achievable as long as the feedback rate is high enough (which scales with the SNR). However, [6] and [7] neglect the temporal correlation of the channels, which can be exploited to further reduce the number of feedback bits [8]–[10]. The authors of [8] propose a differential quantization strategy for MIMO correlation matrices by exploiting the space of symmetric positive-definite matrices. In [9] and [10], unit vector quantization on the Grassmannian manifold is proposed for multi-user broadcast channels and interference channels with time-variant coefficients.

For frame based communication systems the CSI feedback delay can be compensated by channel prediction. In this paper, we tackle the problem of feedback delay compensation by time-variant channel prediction based on limited feedback. We are concerned with low complexity prediction of a fading process whose Doppler bandwidth is much smaller than the communication system's symbol rate. This implies that the fading process can be represented by the weighted sum of a small number of basis functions [11]–[13].

Contribution of this paper:

- For frequency selective SISO interference channels, we show that the basis expansion coefficients can be represented on the Grassmannian manifold building on the concept of [10]. We track and feed back the evolution of the basis expansion coefficients on the manifold and not the channel impulse response as proposed in [10]. This new approach enables channel prediction for delay compensation and allows a further reduction in the number of feedback bits.
- With the basis expansion coefficients, the transmitter is able to recover the channel in advance within the prediction horizon, which greatly reduces the number of feedback bits and yields performance gain in delayed feedback systems.
- We propose a predictive strategy to reduce the difference between two consecutive sets of basis expansion coefficients, which further reduces the quantization error.

II. SYSTEM MODEL

Let us consider a K user frequency selective SISO interference channel, which consists of K transmitter and receiver pairs. The L-tap time-variant impulse response between transmitter j and receiver i is denoted by $\mathbf{h}_{ij}[t] = \left[h_{ij}^1[t], \ldots, h_{ij}^L[t]\right]^{\mathrm{T}}, \forall i, j \in \{1, \ldots, K\}$. Every element $h_{ij}^\ell[t]$ of the channel impulse response is an independent identically distributed (i.i.d.) symmetric complex Gaussian random variable with zero mean and variance p_{ij}^ℓ. Thus, the covariance matrix $\boldsymbol{R}_{\boldsymbol{h}_{ij}} = \mathbb{E}\{\mathbf{h}_{ij}[t]\mathbf{h}_{ij}[t]^{\mathrm{H}}\} = \mathrm{diag}(\left[p_{ij}^1, \ldots, p_{ij}^L\right])$. We assume $\sum_{l=1}^{L} p_{ij}^\ell = 1$. The covariance function per channel tap over consecutive orthogonal frequency division multiplexing (OFDM) symbols $R_h[m] = \mathbb{E}\{\mathbf{h}_{ij}[t]^{\mathrm{H}}\mathbf{h}_{ij}[t+m]\} = J_0(2\pi\nu_{\mathrm{D}}m)$ where J_0 is the 0-th order Bessel function of the first kind and $\nu_{\mathrm{D}} = f_D T_{\mathrm{s}}$ is the normalized Doppler frequency, where f_D denotes the Doppler frequency in Herz and T_{s} denotes the OFDM symbol duration.

We use OFDM to convert the time and frequency selective channel into N parallel time-selective and frequency-flat channels. The $N \times 1$ frequency response is defined as $\mathbf{w}_{ij}[t] = \mathcal{F}_N\{[\mathbf{h}_{ij}[t]^{\mathrm{T}}, \mathbf{0}_{1\times(N-L)}]^{\mathrm{T}}\}$, where $\mathcal{F}_N$ denotes the N-point discrete Fourier transform. The diagonal matrix containing the channel frequency response becomes $\mathbf{W}_{ij}[t] = \mathrm{diag}\left(\mathbf{w}_{ij}[t]\right)$.

For a given transmitter, its signal is only intended to be received and decoded by a single user for a given signaling interval. The signal received at receiver i is the superposition of the signals transmitted by all transmitters, which can be written as

$$\mathbf{y}_i[t] = \mathbf{W}_{ii}[t]\mathbf{x}_i[t] + \sum_{i\neq j} \mathbf{W}_{ij}\left[t\right]\mathbf{x}_j[t] + \mathbf{n}_i[t] \tag{1}$$

where the vector $\mathbf{x}_i[t] \in \mathbb{C}^{N\times 1}$ is the OFDM symbol sent by user i with power constraint $\mathbb{E}\{\mathbf{x}_i[t]^{\mathrm{H}}\mathbf{x}_i[t]\} = PN$. Additive complex symmetric Gaussian noise at receiver i is denoted by $\mathbf{n}_i[t] \sim \mathcal{CN}(0, \mathbf{I}_N)$. We define the SNR as $\mathrm{SNR} = P$.

In this work we consider a user velocity and carrier frequency such that the Doppler bandwidth of the fading process f_D is much smaller than the subcarrier spacing $\Delta f_{\mathrm{sc}} = B/N$ where B is the total bandwidth. Hence, we can assume no inter-carrier interference exists for the processing at the receiver side, please see the discussion in [14, equation (5)] for further details.

A. SISO Interference Alignment with Perfect CSI

We review the concept of IA using the results in [1]. Let us assume that each transmitter and receiver has perfect CSI. Each transmitter i sends a linear combination of d_i symbols along the precoding vectors $\mathbf{v}_i^k$, yielding

$$\mathbf{x}_i[t] = \sum_{k=1}^{d_i} \mathbf{v}_i^k[t] s_i^k[t] \tag{2}$$

where $s_i^k[t] \in \mathbb{C}$ denotes the transmitted symbols and $\mathbb{E}\{\left|s_i^k[t]\right|^2\} = PN/d_i$. The precoding vector $\mathbf{v}_i^k[t]$ fulfills $\left\|\mathbf{v}_i^k[t]\right\|^2 = 1$. According to [1], each transmitter computes the precoding vectors $\mathbf{v}_i^k[t]$ such that the interference signals from the undesired $K-1$ transmitters are aligned at all receivers leaving the interference free subspace for the intended signal. Each receiver i computes, based on its CSI, the postfiltering vectors $\mathbf{u}_i^k[t]$, such that the following interference alignment conditions are satisfied

$$\mathbf{u}_i^k[t]^{\mathrm{H}}\mathbf{W}_{ii}[t]\mathbf{v}_i^\ell[t] = 0, \quad \forall i,\ \forall k \neq l \tag{3}$$

$$\mathbf{u}_i^k[t]^{\mathrm{H}}\mathbf{W}_{ij}[t]\mathbf{v}_j^\ell[t] = 0, \quad \forall i \neq j,\ \forall k,\ l \tag{4}$$

$$\left|\mathbf{u}_i^k[t]^{\mathrm{H}}\mathbf{W}_{ii}[t]\mathbf{v}_i^k[t]\right| \geq c > 0, \quad \forall i,\ k \tag{5}$$

where $\mathbf{u}_i^k[t] \in \mathbb{C}^{N\times 1}$ and $\left\|\mathbf{u}_i^k[t]\right\|^2 = 1$.

B. SISO Interference Alignment with Imperfect CSI

Imperfect CSI results in residual interference [15], thus, IA conditions (3) and (4) can not be satisfied. The authors of [10] and [16] provide an upper bound of average loss in sum rate given imperfect precoders $\hat{\mathbf{v}}_i^k[t]$ and postfilters $\hat{\mathbf{u}}_i^k[t]$

$$\Delta R < \sum_{i,k} \frac{1}{N} \log_2 \left(1 + \frac{\mathbb{E}_{\mathbf{h}}\left[\mathcal{I}_{i,k}^1 + \mathcal{I}_{i,k}^2\right]}{\sigma^2}\right) \tag{6}$$

where

$$\mathcal{I}_{i,k}^1 = \sum_{l\neq k} \frac{NP}{d_i} \left|\hat{\mathbf{u}}_i^k[t]^{\mathrm{H}}\mathbf{W}_{ii}[t]\hat{\mathbf{v}}_i^\ell[t]\right|^2, \tag{7}$$

$$\mathcal{I}_{i,k}^2 = \sum_{j\neq i}\sum_{k=1}^{d_j} \frac{NP}{d_j} \left|\hat{\mathbf{u}}_i^k[t]^{\mathrm{H}}\mathbf{W}_{ij}[t]\hat{\mathbf{v}}_j^\ell[t]\right|^2 \tag{8}$$

denote the inter-stream interference and the inter-user interference respectively. Invoking the results from [6], the last term in (7) and (8) can be upper bounded by

$$\begin{aligned}&\left|\hat{\mathbf{u}}_i^k[t]^{\mathrm{H}}\mathbf{W}_{ij}[t]\hat{\mathbf{v}}_j^\ell[t]\right|^2 \\ &\leq \left\|\mathbf{b}_{i,j}^{k,\ell}[t]\right\|^2 \left\|\mathbf{h}_{ij}[t]\right\|^2 \left(1 - \left|\frac{\mathbf{h}_{ij}[t]^{\mathrm{H}}\hat{\mathbf{h}}_{ij}[t]}{\left\|\mathbf{h}_{ij}[t]\right\|\left\|\hat{\mathbf{h}}_{ij}[t]\right\|}\right|^2\right)\end{aligned} \tag{9}$$

where $\hat{\mathbf{b}}_{i,j}^{k,\ell}[t] = \hat{\mathbf{u}}_i^k[t] \circ \hat{\mathbf{v}}_j^\ell[t]$ represents the Hadamard product of vector $\hat{\mathbf{u}}_i^k[t]$ and $\hat{\mathbf{v}}_j^\ell[t]$, and $\hat{\mathbf{h}}_{ij}[t]$ is the estimate of the time-variant channel impulse response available at the transmitter side. The last term of (9) implies that the actual CSI required for IA is the normalized channel impulse response $\mathbf{h}_{ij}[t]/\left\|\mathbf{h}_{ij}[t]\right\|$. Moreover, the result is rotationally invariant, i.e.

$$\left|\frac{\mathbf{h}_{ij}[t]^{\mathrm{H}}\hat{\mathbf{h}}_{ij}[t]\alpha}{\left\|\mathbf{h}_{ij}[t]\right\|\left\|\hat{\mathbf{h}}_{ij}[t]\alpha\right\|}\right|^2 = \left|\frac{\mathbf{h}_{ij}[t]^{\mathrm{H}}\hat{\mathbf{h}}_{ij}[t]}{\left\|\mathbf{h}_{ij}[t]\right\|\left\|\hat{\mathbf{h}}_{ij}[t]\right\|}\right|^2 \tag{10}$$

where $\alpha \in \mathbb{C}$. As a result, a multiplication with the complex scalar α does not change the signal subspace. Let us define the chordal distance between two unit norm vectors $\mathbf{x}_1$ and $\mathbf{x}_2$ as $d_{\mathrm{c}}(\mathbf{x}_1, \mathbf{x}_2) = \sqrt{(1 - |\mathbf{x}_1^{\mathrm{H}}\mathbf{x}_2|^2)}$. The last term in (9) can be rewritten as $d_{\mathrm{c}}^2(\mathbf{h}_{ij}[t]/\|\mathbf{h}_{ij}[t]\|, \hat{\mathbf{h}}_{ij}[t]/\|\hat{\mathbf{h}}_{ij}[t]\|)$. Hence, to minimize the upper bound in (9), or equivalently the degradation in sum rate as shown in (6) for a limited feedback system, we need a quantization strategy that minimizes the angle, i.e. $d_c(\mathbf{h}_{ij}[t]/\|\mathbf{h}_{ij}[t]\|, \hat{\mathbf{h}}_{ij}[t]/\|\hat{\mathbf{h}}_{ij}[t]\|)$, between the quantized channel impulse response $\hat{\mathbf{h}}_{ij}[t]$ and the true channel impulse response $\mathbf{h}_{ij}[t]$.

III. Reduced-Rank Channel Prediction with Grassmannian Differential Feedback

In this section, we present the reduced-rank channel prediction together with a Grassmannian limited-feedback strategy, which allows the transmitter to recover the future channel realizations in advance. In this work, we consider to separately quantize the channel of different users, thus we drop the user indices i, j to simplify the notation.

A. Reduced-Rank Channel Estimation and Prediction

Let us denote $w^n[t]$, $n^n[t]$ and $x^n[t]$ as the n-th element of the vector $\mathbf{w}[t]$ $\mathbf{n}[t]$ and $\mathbf{x}[t]$ respectively. The channel samples of the n-th subcarrier over time can be written as $\mathbf{g}^n = [w^n[0], \ldots, w^n[M-1]]^{\mathrm{T}}$, where M is the length of a single block. The authors of [12] and [17] show that the channel $\mathbf{g}^n$ can be approximated by a reduced rank representation which expands $\mathbf{g}^n$ by D orthonormal basis functions $\mathbf{u}_p = [u_p[0], \ldots, u_p[M-1]]^{\mathrm{T}}$, $p \in \{0, \ldots, D-1\}$

$$\mathbf{g}^n \approx \mathbf{U}\boldsymbol{\phi}^n = \sum_{p=0}^{D-1} \phi_p^n \mathbf{u}_p \tag{11}$$

where $\mathbf{U} = [\mathbf{u}_0, \ldots, \mathbf{u}_{D-1}]$ collects the basis vectors and $\boldsymbol{\phi}^n = [\phi_0^n, \ldots, \phi_{D-1}^n]$ contains the basis expansion coefficients for the channel $\mathbf{g}^n$. Pilot information interleaved with the data will allow us to obtain noisy channel observations $w'^n[t] = w^n[t] + n'^n[t]$, where $n'^n[t] = n^n[t]x^n[t]^*$ has the same statistical properties as $n^n[t]$. Defining $\mathbf{g}'^n = [w'^n[0], \ldots, w'^n[M-1]]^{\mathrm{T}}$, the estimate of $\boldsymbol{\phi}^n$ is calculated as

$$\tilde{\boldsymbol{\phi}}^n = \mathbf{U}^{\mathrm{H}}\mathbf{g}'^n. \tag{12}$$

In this work, we use the channel prediction method presented in [12] , which employs index-limited discrete prolate spheroidal (DPS) sequences [11] to form the orthogonal basis vectors $\mathbf{u}_p$. The authors of [12] shows that the prediction error of a reduced-rank predictor is mainly dependent on the support of the Doppler spectrum and the shape of the Doppler spectrum is of less importance. Thus, the band-limiting region of the DPS sequences $\mathbf{u}_p[\mathcal{W}]$ is chosen only according to the the support $\mathcal{W}$ of the Doppler spectrum of the time-selective fading process, where $\mathcal{W} = (-\nu_{\mathrm{D}}, \nu_{\mathrm{D}})$ with $\nu_{\mathrm{D}} < 1/2$. To ease notation, we drop $\mathcal{W}$ in the rest of the paper. Given $\mathbf{u}_p$, [12, Sec. 3.D] shows the sequences can be extended over $\mathbb{Z}$ in the minimum-energy band-limited sense. Thus, the predicted channel in the n-th subcarrier at instant $t \in \mathbb{Z}$ is given by

$$\tilde{w}^n[t] = \sum_{p=0}^{D-1} \tilde{\phi}_p^n u_p[t] = \mathbf{f}[t]^{\mathrm{T}}\tilde{\boldsymbol{\phi}}^n \tag{13}$$

where $\mathbf{f}[t] = [u_0[t], \ldots, u_{D-1}[t]]^{\mathrm{T}}$ collects the values of the basis expansion functions at time t.

The energy of the DPS sequences is most concentrated in the interval of the block length M, which is given by

$$\lambda_p = \frac{\sum_{t=0}^{M-1} |u_p[t]|^2}{\sum_{t=-\infty}^{\infty} |u_p[t]|^2} \tag{14}$$

where λ_p is a measure of energy concentration given the support $\mathcal{W}$ of the Doppler spectrum. The values λ_p are clustered near 1 for $p \leq \lceil 2\nu_{\mathrm{D}}M \rceil$ and decay rapidly for $p > \lceil 2\nu_{\mathrm{D}}M \rceil$. The optimal subspace dimension that minimizes the mean square error (MSE) for a given noise level is found to be [12]

$$D_{\mathrm{opt}} = \underset{\mathcal{D}\in\{1,\ldots,M\}}{\arg\min} \left(\frac{1}{|\mathcal{W}|\,M} \sum_{p=\mathcal{D}}^{M-1} \lambda_p + \frac{\mathcal{D}}{MP} \right). \tag{15}$$

B. Achievable DoF with Reduced-Rank Channel Prediction

The MSE per sample is the sum of a square bias and a variance term

$$\mathrm{MSE}[t, D] = \mathrm{bias}^2[t, D] + \mathrm{var}[t, D] \tag{16}$$

where the variance can be approximated by $\mathrm{var}[t, D] = \mathbf{f}[t]^{\mathrm{T}} * \mathbf{f}[t]$. The square bias term is calculated as

$$\mathrm{bias}^2[t, D] = \int_{-\frac{1}{2}}^{\frac{1}{2}} \left| 1 - \mathbf{f}[t]^{\mathrm{T}} \sum_{\ell=0}^{M-1} \mathbf{f}[\ell] e^{-j2\pi\nu(t-\ell)} \right| S_h(\nu)\mathrm{d}\nu \tag{17}$$

where $S_h(\nu)$ denotes the power spectral density of the fading process. Let us define the estimation and prediction error $\mathbf{w}_{\mathrm{e}}[t] = \mathbf{w}[t] - \tilde{\mathbf{w}}[t]$. It is shown in [16] that if $\mathbb{E}\,\|\mathbf{w}_{\mathrm{e}}[t]\|^2 \leq 1/P$, interference alignment with imperfect CSI achieves the same DoF as with perfect CSI. Hence, for frame based communication systems the CSI feedback delay can be compensated by channel prediction. Assuming the prediction range $\mathcal{T}$ is of length T, the DoF can be preserved if the following condition is satisfied

$$\sum_{t\in\mathcal{T}} \mathrm{MSE}[t, D] \leq \frac{T}{PN} \tag{18}$$

where $\sum_{t\in\mathcal{T}} \mathrm{MSE}[t, D]$ decreases with increasing D $\forall D \in [1, \ldots, D_{\mathrm{opt}}]$. If (18) is not satisfied with D_{opt}, the DoF can not be guaranteed for the given prediction range $\mathcal{T}$. On the other hand if D_{opt} satifies (18), the minimum subspace dimension preserving DoF is $D_{\min} \leq D_{\mathrm{opt}}$.

C. Equivalent Delay Domain Representation

We assume the N narrowband channels from the same transmitter receiver pair have the same Doppler bandwidth, thus all N fading processes share the same set of basis expansion functions. Due to the fact $N > L$, the impulse response $\mathbf{h}[t]$ contains much less coefficients than the frequency response $\mathbf{w}[t]$. Thus, $\mathbf{h}[t]$ is better suited for CSI feedback.

The equivalent basis expansion model in the delay domain can be expressed as

$$\left[\tilde{\mathbf{h}}[t]^{\mathrm{T}}, \mathbf{0}_{1\times(N-L)}\right]^{\mathrm{T}} \tag{19}$$

$$= \mathcal{F}_N^{-1}\{\tilde{\mathbf{w}}[t]\}$$

$$= \mathcal{F}_N^{-1}\left\{\left[\mathbf{f}[t]^{\mathrm{T}}\tilde{\boldsymbol{\phi}}^1, \ldots, \mathbf{f}[t]^{\mathrm{T}}\tilde{\boldsymbol{\phi}}^N\right]^{\mathrm{T}}\right\} \tag{20}$$

$$= \begin{bmatrix} \mathcal{F}_N^{-1}\left\{\left[\tilde{\phi}_0^1, \ldots, \tilde{\phi}_0^N\right]\right\} \\ \vdots \\ \mathcal{F}_N^{-1}\left\{\left[\tilde{\phi}_{D-1}^1, \ldots, \tilde{\phi}_{D-1}^N\right]\right\} \end{bmatrix}^{\mathrm{T}} \mathbf{f}[t] \tag{21}$$

$$= [\tilde{\boldsymbol{\gamma}}^1, \ldots, \tilde{\boldsymbol{\gamma}}^L, \mathbf{0}_{D\times N-L}]^{\mathrm{T}}\mathbf{f}[t] \tag{22}$$

where (21) is obtained due to the linearity of Fourier transform and $\tilde{\boldsymbol{\gamma}}^\ell$ is the vector which contains the basis expansion coefficients corresponding to the ℓ-th channel tap $\tilde{h}^l[t]$. We use these delay domain coefficients $\tilde{\boldsymbol{\gamma}}^\ell$ to build up the limited feedback systems.

D. Reformulation of Subspace Representation for the SISO Interference Channels

With the basis expansion coefficients $\tilde{\boldsymbol{\gamma}}^\ell$ estimated from the received block by evaluating (22), the predicted channel impulse response can be written as

$$\tilde{\mathbf{h}}[t] = \begin{bmatrix} \tilde{h}^1[t] \\ \vdots \\ \tilde{h}^L[t] \end{bmatrix} = \begin{bmatrix} \mathbf{f}[t]^{\mathrm{T}}\tilde{\boldsymbol{\gamma}}^1 \\ \vdots \\ \mathbf{f}[t]^{\mathrm{T}}\tilde{\boldsymbol{\gamma}}^L \end{bmatrix} = \underbrace{\begin{bmatrix} \mathbf{f}[t]^{\mathrm{T}} & \mathbf{0}_D^{\mathrm{T}} & \cdots & \mathbf{0}_D^{\mathrm{T}} \\ \mathbf{0}_D^{\mathrm{T}} & \mathbf{f}[t]^{\mathrm{T}} & \cdots & \mathbf{0}_D^{\mathrm{T}} \\ \vdots & \vdots & \ddots & \vdots \\ \mathbf{0}_D^{\mathrm{T}} & \mathbf{0}_D^{\mathrm{T}} & \cdots & \mathbf{f}[t]^{\mathrm{T}} \end{bmatrix}}_{\mathbf{F}[t]} \underbrace{\begin{bmatrix} \tilde{\boldsymbol{\gamma}}^1 \\ \vdots \\ \tilde{\boldsymbol{\gamma}}^L \end{bmatrix}}_{\tilde{\boldsymbol{\Gamma}}} \tag{23}$$

where $\tilde{\boldsymbol{\Gamma}} \in \mathbb{C}^{DL\times 1}$ and $\mathbf{F} \in \mathbb{C}^{L\times DL}$. To show the feasibility of quantizing $\tilde{\boldsymbol{\Gamma}}$, we implicitly assume that perfect channel estimation and prediction is achieved, i.e. $\mathbf{h}[t] = \tilde{\mathbf{h}}[t]$. Inserting the result from (23) into (10) gives $\left|\frac{\tilde{\boldsymbol{\Gamma}}^{\mathrm{H}}\mathbf{F}[t]^{\mathrm{H}}\mathbf{F}[t]\hat{\boldsymbol{\Gamma}}\alpha}{\|\mathbf{F}[t]\tilde{\boldsymbol{\Gamma}}\|\|\mathbf{F}[t]\hat{\boldsymbol{\Gamma}}\alpha\|}\right|^2 = \left|\frac{\tilde{\boldsymbol{\Gamma}}^{\mathrm{H}}\mathbf{F}[t]^{\mathrm{H}}\mathbf{F}[t]\hat{\boldsymbol{\Gamma}}}{\|\mathbf{F}[t]\tilde{\boldsymbol{\Gamma}}\|\|\mathbf{F}[t]\hat{\boldsymbol{\Gamma}}\|}\right|^2$, where $\hat{\boldsymbol{\Gamma}}$ is the quantized version of $\tilde{\boldsymbol{\Gamma}}$. It can be seen that the CSI required for IA is invariant to the norm change and phase rotation of $\boldsymbol{\Gamma}$. Thus the normalized weighting vector $\tilde{\boldsymbol{\Gamma}}/\|\tilde{\boldsymbol{\Gamma}}\|$ also evolves on a Grassmannian manifold $\mathcal{G}_{DL,1}$. Motivated by the idea of Grassmannian differential feedback [10], we propose a strategy to feedback the evolution of $\tilde{\boldsymbol{\Gamma}}/\|\tilde{\boldsymbol{\Gamma}}\|$ instead of the channel impulse responses, which results in a smaller number of feedback bits since the prediction length T is larger than the number of subspace dimension D in general. Furthermore, the channel can be recovered at transmitters in advance to accommodate feedback delay.

E. Grassmannian Differential Feedback with Base Point Optimization

We use $\boldsymbol{\Gamma}_{\mathrm{old}}$ and $\boldsymbol{\Gamma}_{\mathrm{new}}$ to represent the normalized weighting vector for the previous block and the current block. The temporal correlation of the channel results in time correlated weighting vectors, which allows us to connect two consecutive weighting vectors by the shortest curve on the manifold, named geodesic curve. Accordingly, the target point $\boldsymbol{\Gamma}_{\mathrm{new}}$ is reached through the geodesic curve emanating from the base point $\boldsymbol{\Gamma}_{\mathrm{old}}$. The relationship can be defined as [10], [18]

$$\boldsymbol{\Gamma}_{\mathrm{new}} = \boldsymbol{\Gamma}_{\mathrm{old}}\cos(\|\mathbf{e}\|) + \frac{\mathbf{e}}{\|\mathbf{e}\|}\sin(\|\mathbf{e}\|) \tag{24}$$

where $\mathbf{e}$ is the derivative of the geodesic at the base point $\boldsymbol{\Gamma}_{\mathrm{old}}$, also known as tangent vector. It tells the direction and velocity to travel from the based point to the target point and is defined as

$$\mathbf{e} = \arctan\left(\frac{\sqrt{1-|\rho|^2}}{|\rho|}\right)\frac{\frac{\boldsymbol{\Gamma}_{\mathrm{new}}}{\rho} - \boldsymbol{\Gamma}_{\mathrm{old}}}{\frac{\sqrt{1-|\rho|^2}}{|\rho|}} \tag{25}$$

where $\rho = \boldsymbol{\Gamma}_{\mathrm{old}}^{\mathrm{H}}\boldsymbol{\Gamma}_{\mathrm{new}}$. The tangent vector, relating two consecutive vectors on the Grassmannian manifold, can be used to form a differential feedback system. Given the previous quantized weighting vector, the transmitter can compute the new weighting vector according to (24) once the tangent vector is received.

As pointed out in [10], instead of traveling from the previous quantized weighting vector $\hat{\boldsymbol{\Gamma}}_{\mathrm{old}}$ to the current vector $\tilde{\boldsymbol{\Gamma}}_{\mathrm{new}}$, the reconstruction error can be reduced by moving from another point $\acute{\boldsymbol{\Gamma}}_{\mathrm{new}}$, which is closer to $\tilde{\boldsymbol{\Gamma}}_{\mathrm{new}}$. This is known as predictive quantization. However, no prediction is performed in the work of [10]. To improve the quantization accuracy, we consider a predictive strategy which helps to find a close estimate $\acute{\boldsymbol{\Gamma}}_{\mathrm{new}}$ of the target point $\tilde{\boldsymbol{\Gamma}}_{\mathrm{new}}$. Given $\mathbf{U}$, by evaluating (21) and (22) in [12] for each $\mathbf{u}_p$, we can obtain $\acute{\mathbf{U}}$ for $t \in \{T, \ldots, M+T-1\}$. It is a T sample shifted version of $\mathbf{U}$. The predicted basis expansion coefficients are then given by

$$\acute{\boldsymbol{\gamma}}_{\mathrm{new}}^\ell = \underbrace{\mathbf{U}^{\mathrm{H}}\acute{\mathbf{U}}}_{\boldsymbol{\Phi}}\hat{\boldsymbol{\gamma}}_{\mathrm{old}}^\ell, \tag{26}$$

where $\boldsymbol{\Phi} = \mathbf{U}^{\mathrm{H}}\acute{\mathbf{U}}$ is the update matrix. Equation (26) can be viewed as the reevaluation of the basis expansion coefficients accounting for the T predicted channel realizations. Applying (26) to all L delay taps, the predicted weighting vector becomes

$$\acute{\boldsymbol{\Gamma}}_{\mathrm{new}} = \frac{[\acute{\boldsymbol{\gamma}}_{\mathrm{new}}^{1\ \mathrm{T}}, \ldots, \acute{\boldsymbol{\gamma}}_{\mathrm{new}}^{L\ \mathrm{T}}]^{\mathrm{T}}}{\|[\acute{\boldsymbol{\gamma}}_{\mathrm{new}}^{1\ \mathrm{T}}, \ldots, \acute{\boldsymbol{\gamma}}_{\mathrm{new}}^{L\ \mathrm{T}}]\|}. \tag{27}$$

The improvement made by the proposed predictive strategy can be observed in simulation, especially in the operation at high Doppler frequencies. The detailed procedures of the proposed differential feedback scheme are given in algorithm 1 and 2, where t_0 is the absolute time and T_{D} denotes the feedback delay.

Algorithm 1 Quantization at receiver

1: for all $t_0 = 0, T, 2T, \dots$
2: Estimate the basis expansion coefficients using the channel observations received in the interval of $\{t_0 - M + 1, \dots, t_0\}$ using (12), (21) and (22)
3: Stack all the coefficients to form the vector $\tilde{\mathbf{\Gamma}}_{\text{new}}$ as in (23)
4: Calculate the tangent vector between $\acute{\mathbf{\Gamma}}_{\text{new}}$ and $\tilde{\mathbf{\Gamma}}_{\text{new}}$ with (25)
5: Quantize and feedback the quantized tangent vector $\hat{\mathbf{e}}$ according to [10]
6: Reconstruct the weighting vector $\hat{\mathbf{\Gamma}}_{\text{new}}$ with $\hat{\mathbf{e}}$ according to (24)
7: Let $\hat{\mathbf{\Gamma}}_{\text{old}} = \hat{\mathbf{\Gamma}}_{\text{new}}$ and update the base vector to $\acute{\mathbf{\Gamma}}_{\text{new}}$ according to (26) (27)
8: end for

Algorithm 2 Reconstruction at transmitter

1: for all $t_0 = 0 + T_{\text{D}}, T + T_{\text{D}}, 2T + T_{\text{D}}, \dots$
2: Receive the quantized tangent vector $\hat{\mathbf{e}}$
3: Reconstruct the weighting vector $\hat{\mathbf{\Gamma}}_{\text{new}}$ according to (24) and predict channel realizations in range $\{t_0 + T_{\text{D}} + 1, \dots, t_0 + T_{\text{D}} + T\}$ using (13)
4: Let $\hat{\mathbf{\Gamma}}_{\text{old}} = \hat{\mathbf{\Gamma}}_{\text{new}}$ and update the base vector to $\acute{\mathbf{\Gamma}}_{\text{new}}$ according to (26) (27)
5: end for

F. Tangent Vector Quantization

The tangent vector $\mathbf{e}$ can be decomposed into a unit norm direction vector $\mathbf{e}/\|\mathbf{e}\|$ and a tangent magnitude $\|\mathbf{e}\|$. They are considered to be quantized separately. The detailed initialization method and codebooks used for tangent vector quantization are provided in [10]. We use the same approach by minimizing a different function i.e. $d_c(\tilde{\mathbf{\Gamma}}_{\text{new}}, \hat{\mathbf{\Gamma}}_{\text{new}})$.

IV. Simulation Results

In this section, the performance of the proposed scheme is compared to Grassmannian differential feedback (GDF) [10], through Monte-Carlo simulations. Two performance metrics, i.e. the chordal distance between the channels and the sum rate, are evaluated for different numbers of quantization bits and various Doppler frequencies.

We consider a channel with L delay taps and a flat power delay profile i.e. $\mathbb{E}\{\mathbf{h}_{ij}[t]\mathbf{h}_{ij}[t]^{\text{H}}\} = \mathbf{I}_L/L$. Each delay ${h_{ij}}^{\ell}[t]$ is temporally correlated according to Clarke's model [19] with covariance function $\mathbb{E}\{\mathbf{h}_{ij}[t]^{\text{H}}\mathbf{h}_{ij}[t+m]\} = J_0(2\pi\nu_{\text{D}}m)$. The OFDM symbol rate $1/T_s = 1.4 \times 10^4$Hz is chosen according to the 3GPP LTE [20]. A slot with a duration of 0.5ms contains 7 OFDM symbols and two slots form a subframe. The carrier frequency is $f_c = 2.5$GHz.

Fig. 1 shows the average chordal distance (quantization error) for a 3-tap channel, at varying normalized Doppler frequencies $\nu_D \in (0, 7.5\times10^{-3})$, or equivalently a velocity of $v \in (0, 47)$ km/h. For the proposed scheme, we assume exact

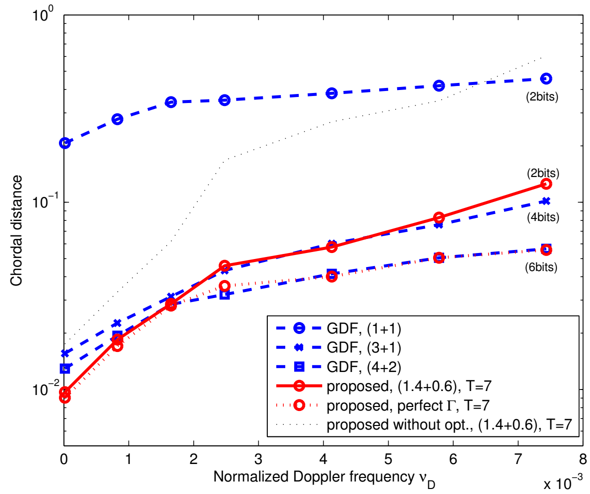

Fig. 1. Average chordal distance versus normalized Doppler frequency ν_D with different number of direction bits and magnitude bits $(a + b)$ per channel realization, compared to GDF [10], the proposed scheme with perfect (unquantized) $\tilde{\mathbf{\Gamma}}$ and the proposed scheme without applying base point optimization (26). The block length $M = 70$. The prediction horizon for our proposed algorithm $T = 7$. The SNR equals 20dB and the number of channel taps $L = 3$. The users are moving at a velocity of $v \in (0, 47)$ km/h.

knowledge of the Doppler frequency ν_D. The varying Doppler frequency results in an optimal subspace dimension change from 1 to 3 according to (15). We employ 10 direction bits and 4 magnitude bits for quantization of the weighting vector $\tilde{\mathbf{\Gamma}}$. The quantized weighting vector is used to predict samples in the range $\mathcal{T} = [M, \dots, M + T - 1]$. For comparison, we apply a minimum mean-square error (MMSE) estimator to the GDF scheme for channel estimation. For both schemes, the channel is observed over $M = 70$ samples. It can be seen that, with 2 bits feedback, the proposed scheme achieves similar performance to GDF with 4 bits feedback per channel realization. Compared to the curve with perfect (unquantized) $\tilde{\mathbf{\Gamma}}$, the performance loss due to quantization is negligible for pedestrian speed and fairly small for moderate speed. Besides, significant improvement is obtained by applying base point optimization (26). Importantly, note that the proposed scheme achieves the above results by *channel prediction*.

The prediction gain can be seen in Fig. 2, which illustrates the sum rate of the three user interference channel over three frequency extensions with feedback delay. The precoders are calculated using the close-form IA algorithm from [1] with the quantized CSI at the transmitters. A feedback delay of $T_{\text{D}} = 1$ms, i.e. the duration of a subframe, is considered $\forall i, j$. We further assume that the delays are known at all transmitters. This makes sense since the delay in the feedback channel can be measured using training signals. Thus, the proposed scheme allow the transmitter to adapt the prediction range to $\mathcal{T} = [M + T_{\text{D}}, \dots, M + T_{\text{D}} + T - 1]$ for delay compensation. By evaluating (18), we can obtain the DoF achievability for a given $\mathcal{T}$ and SNR. It shows that, with the perfect unquantized $\tilde{\mathbf{\Gamma}}$ and the optimal subspace dimension D_{opt}, the proposed scheme achieves perfect DoF for $\mathrm{SNR} < 17\mathrm{dB}$ at $\nu_\mathrm{D} = 0.002$, and $\mathrm{SNR} < 10\mathrm{dB}$ at $\nu_\mathrm{D} = 0.006$. For larger SNR values, the rate gap between the proposed schemes and IA with perfect CSI is increased. It also can be observed that the sum rate loss due to quantization error increases with Doppler frequency ν_D. For $\nu_\mathrm{D} = 0.002$, the performance achieved with quantized feedback and perfect feedback is almost identical. For $\nu_\mathrm{D} = 0.006$, the rate loss due to quantization error increases with SNR, especially for $\mathrm{SNR} > 10\mathrm{dB}$. On the other hand, the non-predictive strategy, e.g. the original GDF scheme, is sensitive to the delay in the feedback channel.

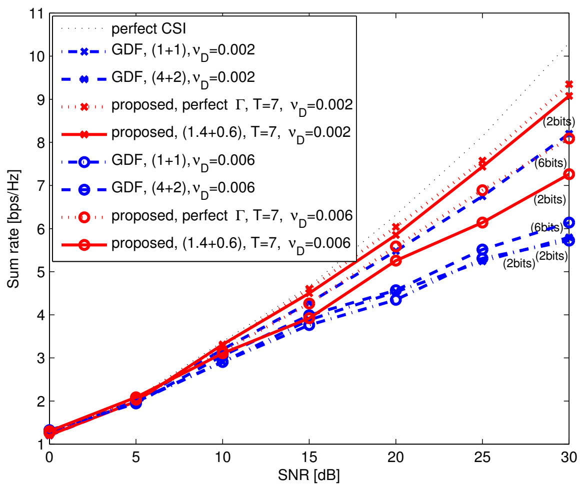

Fig. 2. Sum rate versus SNR with different number of direction bits and magnitude bits $(a+b)$ per channel realization at different normalized Doppler frequency $\nu_D \in \{0.002, 0.006\}$, or a velocity of $v \in \{12.5, 37.5\}$ km/h. The block length $M = 70$. For the proposed scheme, the prediction horizon $T = 7$. The feedback delay $T_\mathrm{D} = 1\mathrm{ms}\ \forall i, j$. The number of channel taps $L = 3$.

V. Conclusion

We developed a limited feedback strategy for channel prediction in the context of SISO interference alignment. Since the time variant channel can be represented by the weighted sum of a few basis expansion functions, we showed that the basis expansion coefficients can be stacked into a vector on the Grassmannian manifold. By feeding back the basis expansion coefficients instead of the channel impulse responses, the number of feedback bits can be reduced. With these coefficients, the transmitter can predict the future channel realizations to compensate for the feedback delay. The proposed scheme yields notable a gain in sum rate with very low rate feedback compared to non-predictive feedback schemes.

Acknowledgment

This work was supported by the project NFN SISE (S10607) funded by the Austrian Science Fund (FWF) as well as the FTW strategic project I-0. The Austrian Competence Center "FTW Forschungszentrum Telekommunikation Wien GmbH" is funded within the program COMET - Competence Centers for Excellent Technologies by BMVIT, BMWFJ, and the City of Vienna. The COMET program is managed by the FFG.

References

[1] V. Cadambe and S. Jafar, "Interference alignment and degrees of freedom of the K-user interference channel," *IEEE Trans. Inf. Theory*, vol. 54, no. 8, pp. 3425 –3441, August 2008.

[2] D. J. Love, R. W. Heath, V. K. Lau, D. Gesbert, B. D. Rao, and M. Andrews, "An overview of limited feedback in wireless communication systems," *IEEE J. Sel. Areas Commun.*, vol. 26, no. 8, pp. 1341–1365, 2008.

[3] K. Gomadam, V. R. Cadambe, and S. A. Jafar, "A distributed numerical approach to interference alignment and applications to wireless interference networks," *IEEE Trans. Inf. Theory*, vol. 57, no. 6, pp. 3309–3322, 2011.

[4] J. H. Lee, W. Choi, and D. J. Love, "On the optimality of opportunistic interference alignment in 3-transmitter MIMO interference channels," *arXiv preprint arXiv:1109.6541*, 2011.

[5] S. A. Jafar, "Exploiting channel correlations-simple interference alignment schemes with no CSIT," in *Proc. Global Telecommunications Conference (GLOBECOM)*, 2010.

[6] H. Bölcskei and I. Thukral, "Interference alignment with limited feedback," in *Proc. International Symposium on Information Theory (ISIT)*, 2009, pp. 1759–1763.

[7] R. T. Krishnamachari and M. K. Varanasi, "Interference alignment under limited feedback for MIMO interference channels," in *Proc. International Symposium on Information Theory (ISIT)*, 2010, pp. 619–623.

[8] D. Sacristán-Murga and A. Pascual-Iserte, "Differential feedback of MIMO channel Gram matrices based on geodesic curves," *IEEE Trans. Wireless Commun.*, vol. 9, no. 12, pp. 3714–3727, 2010.

[9] T. Inoue and R. W. Heath, "Grassmannian predictive coding for delayed limited feedback MIMO systems," in *Proc. 47th Annual Allerton Conference on Communication, Control, and Computing*, 2009, pp. 783–788.

[10] O. El Ayach and R. Heath, "Grassmannian differential limited feedback for interference alignment," *IEEE Trans. Signal Process.*, vol. 60, no. 12, pp. 6481–6494, 2012.

[11] D. Slepian, "Prolate spheroidal wave functions, fourier analysis, and uncertainty—V: the discrete case," *The Bell System Technical Journal*, vol. 57, no. 5, pp. 1371–1430, 1978.

[12] T. Zemen, C. Mecklenbräuker, F. Kaltenberger, and B. H. Fleury, "Minimum-energy band-limited predictor with dynamic subspace selection for time-variant flat-fading channels," *IEEE Trans. Signal Process.*, vol. 55, no. 9, pp. 4534–4548, 2007.

[13] T. Zemen and C. F. Mecklenbräuker, "Time-variant channel estimation using discrete prolate spheroidal sequences," *IEEE Trans. Signal Process.*, vol. 53, no. 9, pp. 3597–3607, September 2005.

[14] T. Zemen, L. Bernado, N. Czink, and A. F. Molisch, "Iterative time-variant channel estimation for 802.11p using generalized discrete prolate spheroidal sequences," *IEEE Trans. Veh. Technol.*, vol. 61, no. 3, pp. 1222–1233, March 2012.

[15] R. Tresch and M. Guillaud, "Cellular interference alignment with imperfect channel knowledge," in *Proc. IEEE International Conference on Communications Workshops*, 2009, pp. 1–5.

[16] O. E. Ayach and R. W. Heath, "Interference alignment with analog channel state feedback," *IEEE Trans. Wireless Commun.*, vol. 11, no. 2, pp. 626–636, 2012.

[17] F. A. Dietrich and W. Utschick, "Pilot-assisted channel estimation based on second-order statistics," *IEEE Trans. Signal Process.*, vol. 53, no. 3, pp. 1178–1193, 2005.

[18] A. Edelman, T. A. Arias, and S. T. Smith, "The geometry of algorithms with orthogonality constraints," *SIAM journal on Matrix Analysis and Applications*, vol. 20, no. 2, pp. 303–353, 1998.

[19] R. H. Clarke, "A statistical theory of mobile-radio reception," *Bell System Technical Journal*, p. 957, July-August 1968.

[20] 3rd Generation Partnership Project (3GPP), *Technical Specification Group Radio Access Network; Evolved Universal Terrestrial Radio Access (E-UTRA); Physical Channels and Modulation (Release 10)*, Std.